

TO THE THEORY OF DEFECTS DETECTION IN PLATE DURING ITS ELECTROMAGNETIC SOUNDING

Z.T. NAZARCHUK and O.I. OVSYANNIKOV

*Karpenko Physico-Mechanical Institute,
Academy of Sciences of Ukraine
5 Naukova Str., Lviv 290601, Ukraine*

ABSTRACT

The general approach to accurate calculation of two-dimensional electromagnetic field scattered by the system of infinitely thin and extended perfectly conducting screens (defects) in dielectric slab is suggested. The slab is situated between two semi-infinite homogeneous half-spaces of different electromagnetic properties and is illuminated by two-dimensional E - or H - polarized electromagnetic wave. The defects system cross-section is supposed to be arbitrary. The integral equations of corresponding diffraction problem are derived and the numerical method of its solving is developed. The integral equations kernels contain the usual free-space Green function and Sommerfeld-type integrals of two variables. The efficient method of the second kernels part evaluation is supposed. Some field calculation results for flat and elliptical cross-sectional defects are presented and discussed.

KEYWORDS

Diffraction theory, planar waveguide, defect, numerical methods, integral equations.

FORMULATION OF INTEGRAL EQUATIONS

Let the slab sides (planes $y = 0$ and $y = -d$) form the interface of media with wave numbers of χ_1, χ_2, χ_3 (Fig.1). The system of cylindrical infinitely thin perfectly conducting defects with cross-section of L_k , $k = \overline{1, N}$ is arbitrary situated in the strip $-d < y < 0$ parallel to Oz -axis. The L_k arcs are supposed as the Lyapunov type contours of arbitrary curvature. The external source of two-dimensional electromagnetic field with the time dependence of $\exp(-i\omega t)$ is irradiated the presented structure. The arising two-dimensional diffraction problem consists in finding of the Helmholtz equation solution, which satisfies the following conditions: of continuity on the media interfaces; of waves absence from infinity (except exciting one); of Dirichlet (E -polarization) or Neumann (H -polarization) on arc L_k , $k = \overline{1, N}$; of Meixner-type near screen ribs (L_k arc end-points). Using the Green function of diffraction problem for a plane-parallel layer, the solution in case of E -polarization is sought as the simple

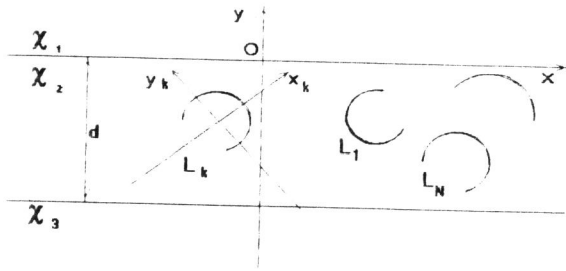


Fig. 1. The cross section of the thin defects system in planar waveguide.

layer potential

$$E(z) = E^*(z) + 2\pi \sum_{k=1}^N \int_{L_k} J_k(t_k) G_E(t_k, z) ds_k. \quad (1)$$

In *H*-case the corresponding representation takes form of the double-layer potential

$$H(z) = H^*(z) + 2\pi \sum_{k=1}^N \int_{L_k} m_k(t_k) \frac{\partial}{\partial n} G_H(t_k, z) ds_k. \quad (2)$$

Here

$$t_k \in L_k, z \notin L_k, G_{E,H}(t, z) \equiv G_{\mathfrak{I}E,H}^1(t, z), \Im\{z\} \geq 0;$$

$$G_{E,H}(t, z) \equiv G_{\mathfrak{I}E,H}^3(t, z), \Im\{z\} \leq -d;$$

$$G_{E,H}(t, z) \equiv G_{\mathfrak{I}E,H}^2(t, z), -d \leq \Im\{z\} \leq 0, z = x + iy,$$

$$G_{\mathfrak{I}E,H}^1(t, z) = \sum_{p=1}^2 \frac{1}{2\pi} \int_0^{\infty} \frac{f_p}{s(s)} e^{\gamma_p \nu_2 - \mathfrak{I}(z)\nu_1} \cos[\xi \Re\{z - t\}] d\xi, \Im\{z\} \geq 0, \quad (3)$$

$$f_1 = 2(\nu_2 p_{13} + \nu_3 p_{23}); \gamma_1 = \mathfrak{I}\{t\}; f_2 = 2(\nu_2 p_{13} - \nu_3 p_{23}); \gamma_2 = -2d - \mathfrak{I}\{t\};$$

$$G_{\mathfrak{I}E,H}^2(t, z) = \frac{i}{4} H_0^{(1)}(\chi_2 r) + S_{\mathfrak{I}E,H}^2(t, z);$$

$$S_{\mathfrak{I}E,H}^2(t, z) = \sum_{p=1}^4 \frac{1}{2\pi} \int_0^{\infty} \frac{g_p}{\nu_2 s(s)} e^{\vartheta_p \nu_2} \cos[\xi \Re\{z - t\}] d\xi, -d \leq \Im\{z\} \leq 0, \quad (4)$$

$$s_1 = (\nu_2 p_{13} - \nu_1 p_{23})(\nu_2 p_{13} + \nu_3 p_{23}); \vartheta_1 = \mathfrak{I}\{t + z\};$$

$$s_2 = (\nu_2 p_{13} - \nu_1 p_{23})(\nu_2 p_{13} - \nu_3 p_{23}); \vartheta_2 = -2d + \mathfrak{I}\{t - z\};$$

$$s_3 = (\nu_2 p_{13} + \nu_1 p_{23})(\nu_2 p_{13} - \nu_3 p_{23}); \vartheta_3 = -2d - \mathfrak{I}\{t + z\};$$

$$s_4 = s_2; \vartheta_4 = -2d - \mathfrak{I}\{t - z\};$$

$$s(s) = (\nu_2 p_{13} + \nu_1 p_{23})(\nu_2 p_{13} + \nu_3 p_{23}) - (\nu_2 p_{13} - \nu_1 p_{23}) \times \\ \times (\nu_2 p_{13} + \nu_3 p_{23}) \exp[-2d\nu_2]; r = |t - z|; p_{ij} = 1 \quad (\text{E-case});$$

$$p_{ij} = \chi_i^2 \chi_j^2 \quad (\text{H-case}); \nu_i = \sqrt{\xi^2 - \chi_i^2}, \Re\{\nu_i\} \geq 0, \mu_i = \mu, i, j = \overline{1, 3},$$

$G_{E,H}$ are the suitable Green function, $\frac{\partial}{\partial n}$ marks the partial derivative by normal at point $t_k = x_k + iy_k$ with arc abscissa s_k of contour L_k , $J_k(t_k)$ and $m_k(t_k)$ are the surface current densities (functions to be find), E^*, H^* are known distribution of the electromagnetic wave excitation, \Re and \Im indicates real and imaginary part of complex value.

At *E*-case we satisfy the Dirichlet conditions on the contours L_k and get the system of integral equations with logarithmic singularity

$$2\pi \sum_{k=1}^N \int_{L_k} J_k(t_k) G_{2E}^2(t_k, t_l^0) ds_k = -E^*(t_l^0), \quad (5)$$

$$t_k \in L_k, t_l \in L_l^0, l = \overline{1, N}.$$

At *H*-polarized excitation in a similar manner we obtain the system of singular integrodifferential equations

$$2\pi \frac{\partial}{\partial n_0} \sum_{k=1}^N \int_{L_k} m_k(t_k) \frac{\partial}{\partial n} G_E(t_k, z) ds_k = -\frac{\partial}{\partial n_0} H^*(t_l^0), \quad (6)$$

$$t_k \in L_k, t_l^0 \in L_l, l = \overline{1, N}.$$

Numerical solution of these systems we'll obtain by the variant of mechanical quadratures method which Panasyuk et al.(1984) supposed.

NUMERICAL SOLUTION OF INTEGRAL EQUATIONS

Let the contours $L_k, k = \overline{1, N}$ are described parametrically

$$t_k = t_k(\tau), \tau = [-1; 1] \quad (7)$$

by complex-valued functions of real parameter τ . As we have $ds_k^0 = |t_k'(\tau)| d\tau$ we can rewrite the equations (5) and (6) at segment $[-1, 1]$ in normalized form. Then we can apply the necessary quadrature formulae (Nazarchuk, 1989) which take into consideration the integrands singularities. When this is done, we obtain the system of linear algebraic equations in nodal points for each of wave polarization. To achieve the algorithm effectiveness we use the subsequent accounting procedure of the wave rereflection from defects.

Numerical evaluation of Green functions (3) and (4) must be done with care but it is routine. When $|\Re\{t_k - t_l^0\}|$ is large, their integrands are highly oscillatory and cause the integrals to be difficult to evaluate numerically. Under this condition it is convenient to convert these integrals (determined over the real axis in ξ -plane) to integrals along contour Γ (see Fig.2). For additional computer time decrease during oscillatory

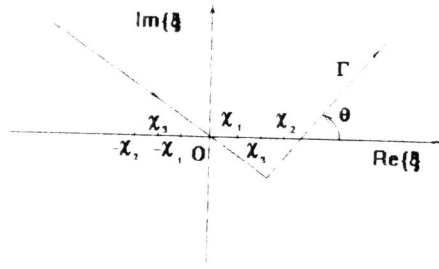


Fig. 2. The integration contour in ξ -plane.

integrals evaluation we build for them the Lagrange type interpolation polynomial of two parameters

$$I(\alpha, \beta) = \omega(\alpha, \beta) \frac{T_{m_1}(\tau) T_{m_2}(\zeta)}{m_1 m_2} \sum_{k=1}^{m_1} \frac{T_{m_1-k}(\tau_k)}{\tau_k - \tau} \times \quad (8)$$

$$\times \sum_{l=1}^{m_2} \frac{T_{m_2-l}(\zeta_l)}{\zeta_l - \zeta} I^*(\alpha^* \tau_k, \beta^* \zeta_l) =$$

$$= \omega(\alpha, \beta) \frac{T_{m_1}(\tau) T_{m_2}(\zeta)}{m_1 m_2} \sum_{k=1}^{m_1} \frac{1}{\tau_k - \tau} \sum_{l=1}^{m_2} \frac{1}{\zeta_l - \zeta} I_0^*(\alpha^* \tau_k, \beta^* \zeta_l),$$

$$\tau = \alpha/\alpha^*, \zeta = \beta/\beta^*, \tau_k = \cos \left[\frac{2k-1}{2m_1} \pi \right], \zeta_l = \cos \left[\frac{2l-1}{2m_2} \pi \right], -1 \leq \tau, \zeta \leq 1,$$

$$T_n(\tau) = \cos [n \arccos(\tau)].$$

Here α^* and β^* are the greatest values of the parameters α and β , which are need to solve of the integral equations system, $\omega(\alpha, \beta)$ function is proportional to Sommerfeld-type integral asymptotic behavior. In our case $\omega(\alpha, \beta) = \exp[i\chi|\alpha + i\beta|]$. The functions $I^*(\alpha^* \tau_k, \beta^* \zeta_l)$ and $I_0^*(\alpha^* \tau_k, \beta^* \zeta_l)$ we define from the relations

$$I(\alpha, \beta) = \omega(\alpha_k, \beta_l) I^*(\alpha^* \tau_k, \beta^* \zeta_l), \quad (9)$$

$$I(\alpha, \beta) = \omega(\alpha_k, \beta_l) I_0^*(\alpha^* \tau_k, \beta^* \zeta_l) T_{m_1-k}(\tau_k) T_{m_2-l}(\zeta_l),$$

$$\alpha_k = \alpha^* \tau_k, \beta_l = \beta^* \zeta_l, k = \overline{1, m_1}, l = \overline{1, m_2}.$$

One time numerically calculating values $I_0^*(\alpha^* \tau_k, \beta^* \zeta_l)$, formula (8) gives the possibility to obtain an effective algorithm of integral evaluation at arbitrary arguments τ and ζ .

RESULTS AND OBSERVATIONS

The numerical solution method of the previous section has been employed to determine the field on the interface $y = 0$ and at $x \rightarrow \pm\infty$ (wave zone or far-field pattern). Let's consider the particular case when excitation are the plane wave

$$W^*(z) = e^{-i\chi_1 z}, \quad (10)$$

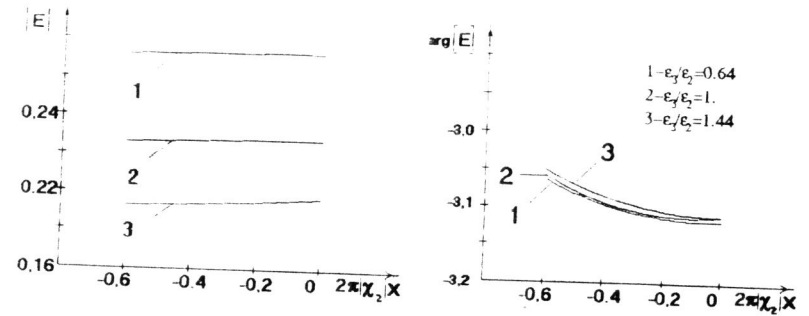


Fig. 3. The magnitude and phase dependencies at different dielectric permeabilities of the underlying halfspace (the case of plane E - wave scattering).

or the own waveguide mode

$$W^*(z) = \begin{Bmatrix} \cos \\ \sin \end{Bmatrix} p_j \chi_2 (y - d/2) e^{h_j \chi_2 z}, -d \leq y \leq \chi_1 = \chi_2. \quad (11)$$

($2\pi/(h_j \chi_2)$ is the waveguide mode wavelength; $p_j = \sqrt{\epsilon^2 - h_j^2}$). The symbol W^* marks E^* in E - case or H^* in H -case.

Let the relation $\chi_1/\chi_2 = 0.1$ occurs. The single metallic strip is situated in the slab at $y = -d/2$. We consider an important problem of the slab properties influence at the scattered electromagnetic field. At Fig.3 and Fig.4 we present the magnitude and phase dependencies when E -polarized plane wave is scattered. It has been shown that under slight variation both of the layer thickness and dielectric permeability of underlying halfspace the scattered wave amplitude undergoes substantial changes too. Its phase remains almost unchanged in this case. According to the phase dependence one can find a defect, determine its shape and the depth of occurrence.

The given below numerical results correspond to the configuration shown in Fig.5. Calculations were carried out during plate sounding both by E - and H -polarised non attenuated planar waveguide mode. In this case the conditions of the maximum electromagnetic energy dissipation in the surrounding space have been established. Let $\chi_1 = \chi_2$ and $1.5\chi_1 = \chi_2$. In the parallel-plate region the transmitted and reflected power magnitudes being normalized by the incident mode power respectively define the transmission ($T^2 = P^t/P^{inc}$) and reflection ($R^2 = P^r/P^{inc}$) coefficients as well as the dissipated out energy ($E = 1 - T^2 - R^2$). The parametrical equations of contours L_k in this case are described by formula

$$t_k(\tau) = a \cos((\pi - \vartheta)\tau) + ie \sin((\pi - \vartheta)\tau) e^{ia - id/2 + (2a + l)(k-1)}, \quad (12)$$

$$-1 \leq \tau \leq 1, k = \overline{1, 2},$$

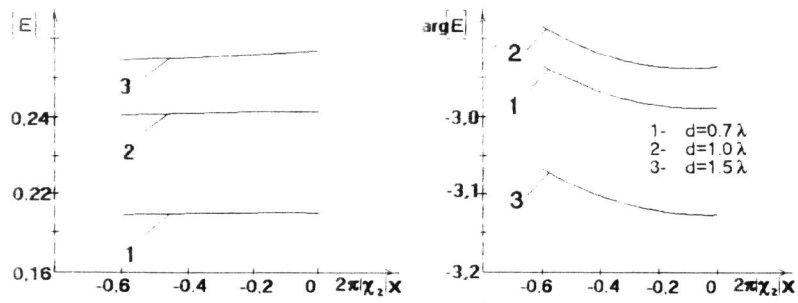


Fig. 4. The magnitude and phase dependencies at different slab thickness (the case of plane *E*- wave scattering).

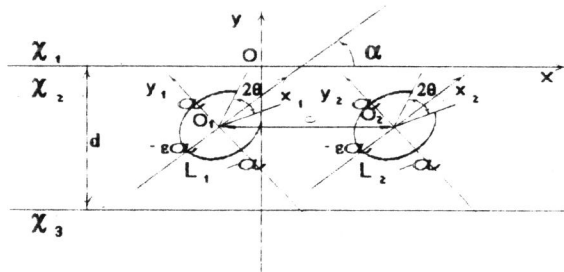


Fig. 5. Cross section of elliptical screens in the planar waveguide.

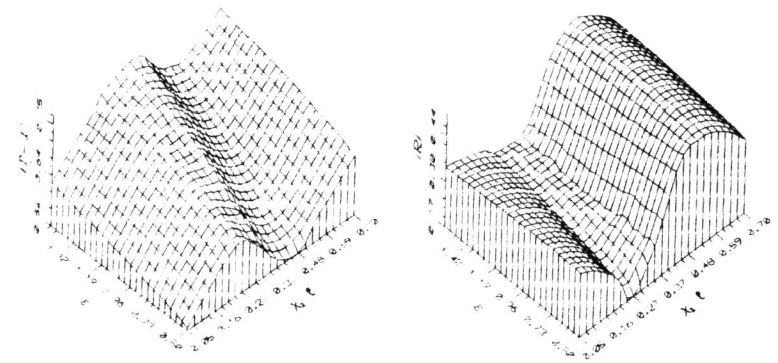


Fig. 6. Transmission and reflection of the *E*- polarized wave as distance $\chi_2 l$ and curvature ϵ functions.

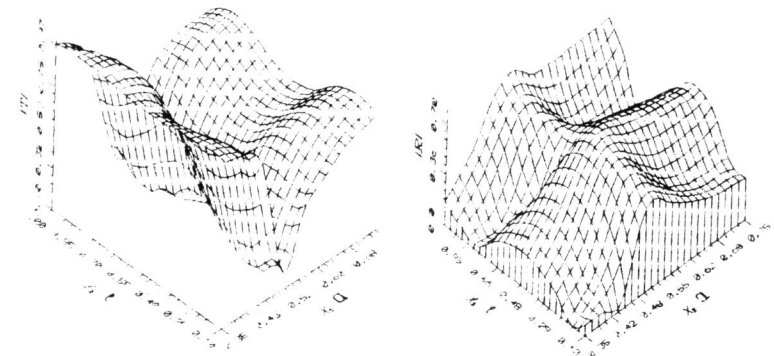


Fig. 7. Transmission and reflection of the *H*-polarized wave as distance $\chi_2 l$ and defects size $\chi_2 a$ functions.

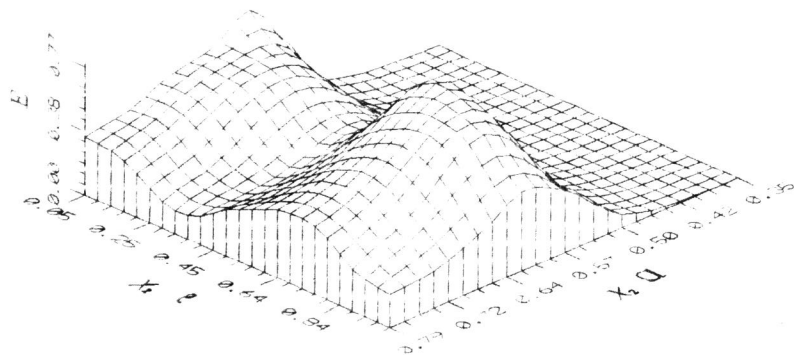


Fig. 8. The H -polarized wave energy dissipation as the function of distance $\chi_2 l$ and size $\chi_2 a$.

where a and ϵa are the ellipses half-axis, l -distance between screens. In the E -case we put $\chi_2 a = 0.35$, $\alpha = \pi/2$, $\vartheta = \pi$. In the H -case we assume $\alpha = \pi/6$, $\vartheta = \pi/6$, $\epsilon = 0.6$. In Fig.6 the E -polarized wave transmission and reflection coefficients as functions of distance between screens $\chi_2 l$ and their curvature ϵ are shown. The functions maximums depend on distance between screens and parameter ϵ (change of curvature ϵ is equivalent to change of screens size). Note that location of the functions maximums depend on ϵ weakly. For small curvature ϵ the transmission maximum we observe at $l \approx 0.4\lambda$ and minimum - at $l \approx 0.27\lambda$ (λ - is wavelength). Increase of the screens size causes the functions $|T - 1|$ and $|R|$ extremes shift to high frequency range. The results of H -polarized scattered field calculations as function on distance $\chi_2 l$ and screens size $\chi_2 a$ are performed in Fig.7 and Fig.8. We can see that value $\chi_2 a = 0.52$ which corresponds to resonance size of each screen remain extremely in the case of its system. The resonance amplitude depends on the distance between defects weakly. The largest and smallest transmission coefficient values are achieved at $\chi_2 a = 0.48$ and 0.21 . The transmission resonance at $l \approx 0.48\lambda$ corresponds to waves rereflection by screens system. The resonance amplitude depends on the screens size only if $\chi_2 a \leq 0.55$. The corresponding analysis of energy dissipation (Fig.8) shows that the single defect resonance is the reason of powerful energy dissipation and the screens system decreases this losses.

REFERENCES

- Nasarchuk Z.T. (1989) Numerical Investigation of Waves Diffraction by Cylindrical Structures.- Naukova Dumka Publ. House.- Kiev (in Russian).
 Panasyuk V.V., Savruk M.P., Nasarchuk Z.T. (1984) Method of Singular Integral Equations in Two-Dimensional Diffraction Problems.- Naukova Dumka Publ. House.- Kiev (in Russian).

THEORETICAL STUDY ON PECULIARITIES OF SMALL ELLIPSOIDAL DEFECTS DETECTING AND EVALUATION IN LAYERED MEDIAS

A. ORLOWSKY

G.V. Karpenko Physico-Mechanical Institute
 5 Naukova St., Lviv 290601, Ukraine

ABSTRACT

On the basis of the equivalent sources method the small defect with its maximal dimension more less than electromagnetic wave length in the material under evaluation are substituted by electric and magnetic dipoles. Equivalent dipole moments are presented as a product of a polarizability tensor and field intensity vector at the defect coordinate. Such representation allows the analysis of the defect shape and orientation influence upon scattered field to reduce to the polarizability tensor investigation. Numerical analysis of the dependence of the void spheroidal defect shape and orientation upon equivalent dipole moment has been carried out.

KEYWORDS

Equivalent sources method, equivalent electric dipole, layered media, ellipsoidal defect, nondestructive testing.

THEORETICAL BACKGROUND

Dipole Model. For the case of small defects while $a \ll \lambda$, in which a is the greatest defect dimension and λ is a wavelength in the material with defect, scattered field with sufficient for the practical purposes accuracy is described by a dipole model. Such mathematical model results from the equivalent sources method in which small defect is substituted by sum of the electric and magnetic dipoles with orientation depending on defect shape and orientation and primary electromagnetic field electric and magnetic intensity vectors direction. Besides dipoles moment value depends upon defect and media electric and magnetic permeability correlations (Senior, 1976). Then the problem is reduced to three independent subproblems: